

# Laser Based Measurement for the Monitoring of Shaft Misalignment

Anthony Simm<sup>a</sup> Qing Wang<sup>a1</sup> Songling Huang<sup>b</sup> Wei Zhao<sup>b</sup>

<sup>a</sup>School of Engineering and Computing Sciences, Durham University, United Kingdom.

<sup>b</sup>State Key Laboratory of Power Systems, Department of Electrical Engineering, Tsinghua University, Beijing, China

## Abstract

This paper presents a method for real-time online monitoring of shaft misalignment, which is a common problem in rotating machinery, such as the drive train of wind turbines. A non-contact laser based measurement method is used to monitor positional changes of a rotating shaft in real time while in operation. The results are then used to detect the presence of shaft misalignment. An experimental test rig is designed to measure shaft misalignment and the results from the work show that the technique can be used for the monitoring of both offset and angular shaft misalignment, which will have applications in the condition monitoring and maintenance of various types of rotating machinery.

**Keywords:** Condition monitoring, Shaft misalignment, Laser distance measurement

## 1 Introduction

When performing maintenance on machinery, the following techniques are common: 1) run to failure where a piece of equipment must fail before any maintenance is performed; 2) preventative (or periodic) maintenance where maintenance is based on the length of the operating period, using criteria such as the mean time to failure (MTTF) measurement for the machine; 3) predictive maintenance where the operating condition of the machine is monitored to identify the need for repairs through data analysis and diagnosis [1].

Predictive maintenance strategies have led to the need for machinery condition monitoring. Condition monitoring can be defined as monitoring the physical parameters associated with the operation of the machine, such as vibration, temperature or pressure, to determine the operational condition of the machine. Improvements in maintenance strategies have economic benefits through improved production and less downtime, as well as indirect benefits through the need for fewer spare parts [2]. Examples of previous research on condition monitoring for rotating machines use vibration sensors for the monitoring of bearings to identify shaft rub and shaft misalignment [3], fault diagnosis using the empirical mode decomposition method [4] and acoustic noise measurements to predict the remaining useful life of a machine [5].

A typical application of condition monitoring for rotating machines is in wind turbines [6], specifically in offshore wind turbines, due to inaccessible locations [7], which may be expensive or difficult to access, with variable operating conditions. The drive train of the wind turbine consists of typically, a low speed shaft (on the rotor side), a gearbox, and a high-speed shaft (on the generator side) as well as support bearings, one or more couplings (between the shaft and the gearbox) and a mechanical brake [8]. A study [9] showed that 25% of the operational expenditure for an offshore wind farm is for operation and maintenance activities so any improvement in monitoring, leading to a reduction in maintenance costs, could eventually drive down the cost of energy.

---

<sup>1</sup> Corresponding Author. Tel.: 0044 191 334 2381, Fax: 0044 191 334 4208.  
Email address: qing.wang@durham.ac.uk

## 2 Shaft misalignment

A shaft is an essential part of the rotating machine; it is used to transmit power and motion. A common problem (estimated to cause over 70% of vibration problems [10]) in rotating machinery is shaft misalignment. Shaft misalignment occurs when the centre lines of rotation of two (or more) machinery shafts are not in line with each other [11]. This increases axial and radial forces on bearings, seals and couplings, increasing the amount of wear in these components, leading to an increase in vibration in the machine and bearings, it also increases bending of the shaft, increasing the risk of shaft failure and reducing the amount of power transmitted through the shaft [12]. Even if initially, or after adjustment, the shaft is aligned, during operation various factors such as thermal growth, piping pressure and foundation movements will alter the alignment [13].

Previous work on shaft misalignment monitoring has mainly been focused on looking at the vibration response. Arebi *et al.* [14] developed an on-line misalignment monitoring system using a wireless accelerometer mounted directly to the shaft, to measure the acceleration due to vibration. Work in rotor-dynamics shows that shaft misalignment caused by rotor imbalance leads to synchronous vibrations (frequency of vibration at twice the shaft speed) [15]. Dewell and Mitchell showed that the response to a misaligned coupling contained vibration frequencies of two times and four times the rotation speed [16], Xu and Marangoni also showed vibration frequencies at multiples of rotation speed [17, 18]. Patel and Darpe [10] describe a drawback in using vibration monitoring to monitor for shaft alignment, as shaft damage, shaft stiffness and the type of coupling used can also affect vibration response. Shaft misalignment should cause vibration in both the connected machines, if it is only on a single machine, this could indicate other problems such as a cracked case [19]. As well as using vibration measurements, analysis of the motor current has been applied to shaft misalignment monitoring, Chaudhury and Gupta [20] and Verma *et al.* [21] used spectral characteristics of the stator current to identify shaft misalignment, Thomson and Fenger used motor current signature analysis to identify faults such as misalignment [22]. Similarly to the work on vibration measurements, Bossio *et al.* showed that angular misalignment has an effect on current at frequencies of two times the rotation frequency [23].

As well as measuring the response of the motor (current) or shaft (vibration) directly, indirect methods have been used to identify shaft misalignment. Rameshkumar *et al.* investigated the effect of misalignment on “coast down time” (time between the power cut off and the machine stopping rotating). They found that as shaft misalignment increased, the coast down time decreased, due to the increased power loss caused by the shaft misalignment and increased torque on the bearings [24]. Strain gauges have also been used to measure the presence of misalignment on turbine rotors [25] and to measure the increased gear loading caused by shaft misalignment [26]. Fulzele *et al.* used an optical sensor to measure shaft vibration by measuring the fluctuation of reflected light from the shaft [27]. Various methods have been developed to model or predict shaft misalignment; Sekhar and Prabhu used Finite Element Method (FEM) modeling to investigate the effect of coupling misalignment on the vibration response of a rotor-bearing system [28]. Cho *et al.* [29] and Fang *et al.* [12] used principal component regression (PCR) and partial least squares (PLS) to predict shaft parallel and angular misalignment. Yang and Tavner used empirical mode decomposition to reconstruct shaft orbit measurements to identify shaft misalignment [30].

Monitoring of shaft alignment during operation is needed as an effective tool in maintenance. A survey on rotating machinery in industry [31] showed that fewer than 10% of 160 machines examined were within acceptable shaft alignment, also 30% of a machine's down time is due to poor alignment [32]. Shaft misalignment consists of three types [33]:

- 1) Offset where the two shafts are on two separate parallel centerlines (Figure 1a).

- 2) Angular where the two shafts are coaxial but at an angle to each other (Figure 1b).
- 3) In reality, shaft misalignment would be a combination of both of these effects (Figure 1c).

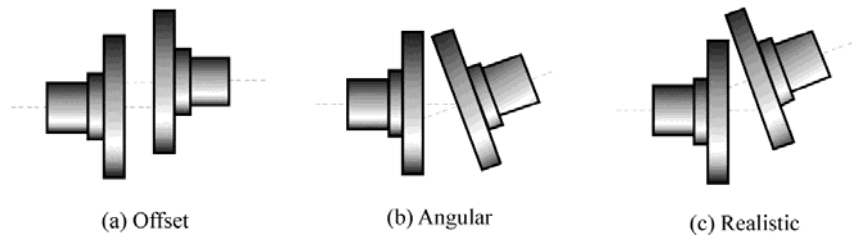


**Figure 1 Types of shaft misalignment**

Offset misalignment affects power consumption more than angular misalignment and the components of misalignment are additive irrespective of whether they are horizontal or vertical [31]. The process of shaft alignment is the positioning of the shaft centre lines of the driver machine and driven machine to create collinear shafts, where the rotational centre lines of the coupled shafts are parallel and intersect (like a single shaft), this is accomplished through either shimming or moving the machine.

To measure the amount of shaft misalignment, the following methods are commonly used:

- 1) Straight edge (Figure 2a).
- 2) Dial indicator (reverse indicator method shown in Figure 2b).
- 3) Laser indicator (Figure 2c).

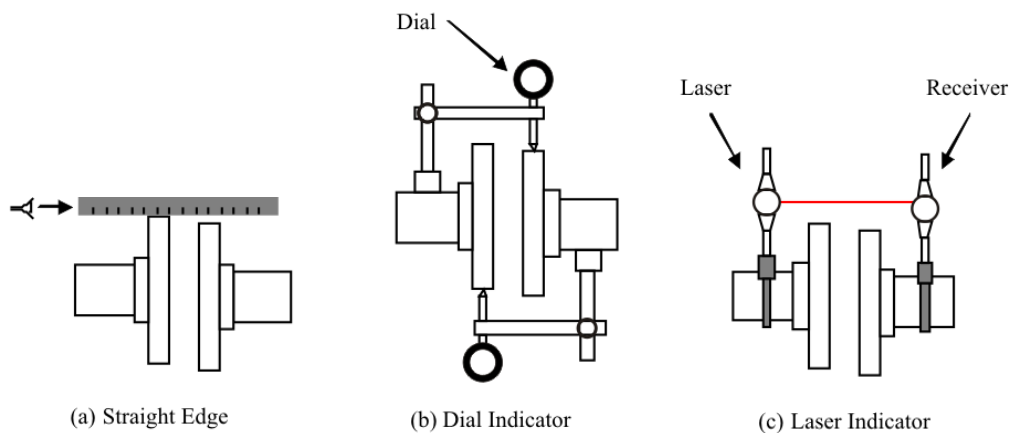


**Figure 2 Misalignment measurement methods**

The straight edge is usually the first stage of inspection to get an approximate reading before moving onto the more accurate methods. The common method is to use dial indicators. Recently, these have been replaced by laser based misalignment measurement methods, which are more accurate and can be automated to calculate the amount of shaft misalignment automatically.

Monitoring and predicting the shaft alignment condition is important for making decisions on when to perform maintenance of the rotating machine, by counting misalignment events or using the measurements to identify other fault types such as bearing damage. This work proposes an alternative to the previously mentioned shaft misalignment measurement methods: a non-contact laser based measurement technique to capture the on-line positional changes of a shaft, for improved shaft misalignment monitoring.

### 3 Experimental study

The most common method to counteract the presence of shaft misalignment is to use a coupling, where the coupling is inserted between the driving and driven shafts. Couplings are chosen based on various factors such as environment, vibration and stiffness [34]. The two main types of coupling are: 1) metallic, such as, chain, gear and disc couplings, which have high stiffness and tolerance to extreme environments and 2) elastomeric, such as, pin and bushing, jaw and sleeve couplings, which are torsionally soft and have vibration damping/shock absorbing qualities. In this work a set of huco elastomeric d-loop couplings are used, due to a large range of permissible operating misalignment ( $10^\circ$  angular misalignment and 2.6mm offset misalignment) [35], allowing for a range of shaft misalignment to be examined.

#### 3.1 Test rig design

To simulate a rotating drive train, an experimental test rig has been designed, as shown in Figure 3. The laser based measuring method is designed to be non-contact, so it can be easily applied to various types of rotating machinery. Laser distance measurements have engineering applications in areas such as vibrometry [36], coordinate measurement systems [37] and micro displacement measurement [38]. Laser mouse sensors have also been used for non-contact shaft speed measurements [39], as an alternative to electromagnetic sensors.

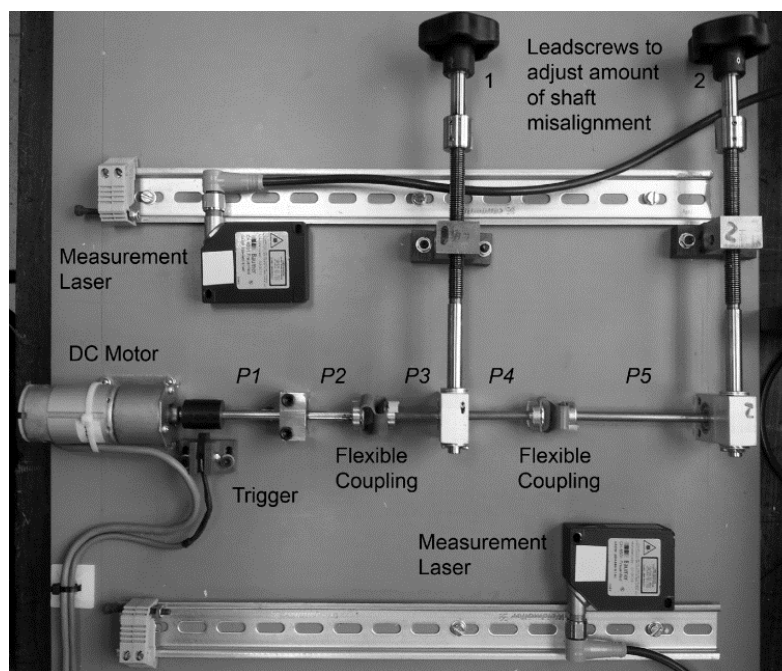


Figure 3 Experimental test rig

A Baumer photoelectric distance measuring sensor with a measuring range of 30mm to 130mm, a resolution of 0.06mm and a response time of less than 10ms, is used to measure the amount of shaft misalignment present by measuring shaft positional changes (the distance from the laser to the shaft). The laser uses optical triangulation, where a pulsed red laser line is projected onto the surface of the shaft and part of the reflected light is measured using a photodiode detector, where the angle of incidence is used to calculate the distance.

The motor is used to rotate the shaft (~37rpm) and an optoelectronic trigger is used to measure shaft rotation for ensemble averaging. The 6mm diameter steel shaft is supported by support bearings that are attached to lead screws (~1.25mm pitch) to give adjustable amounts of shaft misalignment (both offset and angular). Note that *P1-P5* are shaft misalignment measuring positions.

The first stage in a condition monitoring system is to acquire and process the data related to the condition of the machine [40]. The data acquisition is performed using a National Instruments USB-6218 card. The data acquisition software is developed using DAQmx drivers built into LabVIEW 2012. This software allows control of the motor speed and acquisition of the trigger signal and output from the two measurement lasers. Data from these measurements will allow the monitoring of any ongoing shaft misalignment from the changes in the distance measurement over time, an improvement over existing offline maintenance methods to monitor shaft misalignment [11]. The data is sampled at 300Hz to avoid Nyquist issues with the 10ms laser response time and 10 seconds of data are recorded. The data is then processed to give an estimation of real time shaft misalignment.

### 3.2 Shaft misalignment tests

To investigate the monitoring of shaft misalignment using the experimental test rig, the following tests were performed:

- 1) Test one: Increase misalignment using lead screw one by one revolution (offset measured at 1.46mm).
- 2) Test two: Increase misalignment using lead screw one by two revolutions (offset measured at 2.36mm).
- 3) Test three: Increase misalignment using lead screw two by one revolution (offset measured at 0.57mm).
- 4) Test four: Increase misalignment using lead screw two by two revolutions (offset measured at 1.18mm).
- 5) Test five: Increase misalignment using both lead screw one and lead screw two both by one revolution.
- 6) Test six: Increase misalignment using both lead screw one and lead screw two both by two revolutions.
- 7) Test seven: Continuously increase the amount of misalignment using lead screw one and measure as it changes dynamically over time.

### 3.3 Data processing

The data is acquired as a voltage measurement from the lasers. It is converted to a distance using the relationship,  $Distance(mm) = 23.2 \times Voltage(V) + 4.92$ , from the line fitted to the

measurement data shown in Figure 4. For example, a laser output of 1.5V equates to a distance of 39.72mm.

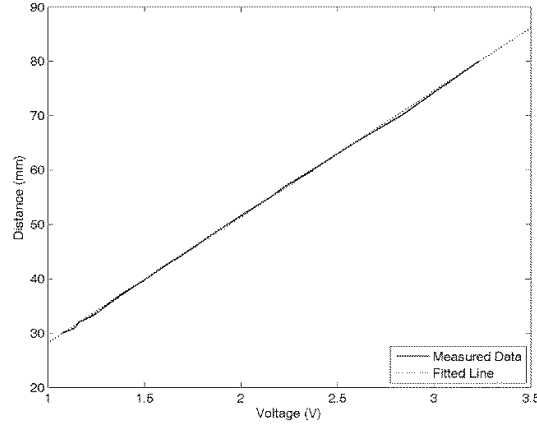


**Figure 4 Laser distance calibration**

To remove noise from the data, the measurement is filtered using a weighted moving average filter from the LabVIEW Advanced Signal Processing Toolkit [41]. In this case, all of the data is read in and then the moving average filter operation is applied to smooth the data as shown in (1).

$$\begin{aligned}
 y(n) &= a_0x(n) + a_1x(n+1) + \dots + a_qx(n+q) \\
 &= \sum_{r=0}^q a_r x(n+r).
 \end{aligned} \tag{1}$$

Where  $x$  is the vector of input data,  $y$  is the vector of filtered data and  $a_r$  is a set of user-defined weights. In this case a Henderson 23-term moving average filter is used [42], here the number of weights must be odd, the weight array must be symmetric and  $\sum a_r = 1$  as shown in (2).

$$\begin{aligned}
 y(n) &= -0.00428 x(n) - 0.01092 x(n+1) - 0.01569 x(n+2) - 0.01453 x(n+3) \\
 &\quad - 0.00495 x(n+4) + 0.01343 x(n+5) + 0.03893 x(n+6) + 0.06830 x(n+7) \\
 &\quad + 0.09740 x(n+8) + 0.12195 x(n+9) + 0.13832 x(n+10) + 0.14406 x(n+11) \\
 &\quad + 0.13832 x(n+12) + 0.12195 x(n+13) + 0.09740 x(n+14) + 0.06830 x(n+15) \\
 &\quad + 0.03893 x(n+16) + 0.01343 x(n+17) - 0.00495 x(n+18) - 0.01453 x(n+19) \\
 &\quad - 0.01569 x(n+20) - 0.01092 x(n+21) - 0.00428 x(n+22)
 \end{aligned} \tag{2}$$

The result of filtering the measurement data to smooth the data and remove outliers is shown in Figure 5. The dotted lines show the limit for outlier data (unusual values of data), in this case 1.5 times the interquartile range (middle 50% of the values in the data) [43].

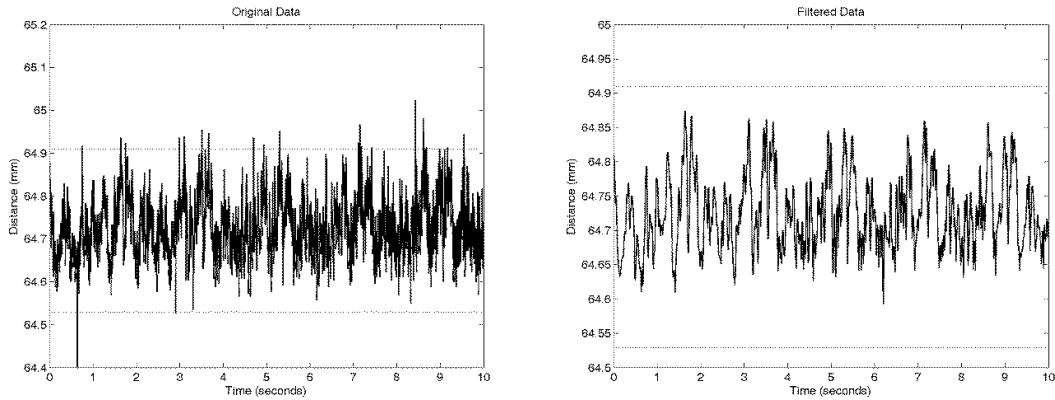


**Figure 5 Filtered data**

The mean value will then be used for distance calculations, in the example in Figure 5, the mean of both the original data and filtered data is 64.72mm, showing that in this case filtering removes extreme values with no change to the mean.

When the data has been processed the mean over the periodic results (the revolutions of the shaft) can be calculated using the ensemble average. The difference between time average and ensemble average is shown in Figure 6.

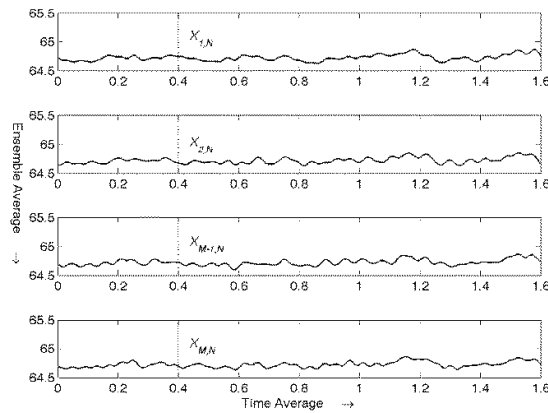


**Figure 6 Types of averaging**

If  $X_{i,j}$  is the  $j$ th time element in the  $i$ th revolution the ensemble can be represented using the matrix in (3) [44].

$$\begin{array}{cccccc}
 & & & \text{time} & & \\
 & & & \rightarrow & & \\
 & \mathbf{X}_{1,1} & \mathbf{X}_{1,2} & \dots & \mathbf{X}_{1,N-1} & \mathbf{X}_{1,N} \\
 & \mathbf{X}_{2,1} & \mathbf{X}_{2,2} & \dots & \mathbf{X}_{2,N-1} & \mathbf{X}_{2,N} \\
 \text{revs} \downarrow & \vdots & \vdots & \ddots & \vdots & \vdots \\
 & \mathbf{X}_{M-1,1} & \mathbf{X}_{M-1,2} & \dots & \mathbf{X}_{M-1,N-1} & \mathbf{X}_{M-1,N} \\
 & \mathbf{X}_{M,1} & \mathbf{X}_{M,2} & \dots & \mathbf{X}_{M,N-1} & \mathbf{X}_{M,N}
 \end{array} \tag{3}$$

With  $N$  columns of evenly spaced time samples ( $300\text{Hz} = 3.33\text{ms}$ ) and  $M$  rows of time series for each shaft revolution. For the  $i$ th revolution it is possible to compute the time average denoted by  $\bar{X}$ , given by (4) [44].

$$\bar{X}_{i,j} = \frac{1}{N} \sum_{j=1}^N X_{i,j} \tag{4}$$

Similarly for the  $j$ th sample, the ensemble average, denoted by  $\langle X \rangle$ , can be calculated over all rotations given by (5) [44].

$$\langle X_{i,j} \rangle = \frac{1}{M} \sum_{i=1}^M X_{i,j} \tag{5}$$

To identify the start of each shaft revolution, a trigger signal is used as shown in Figure 7, where the start and end of each rotation is denoted with an “X”.

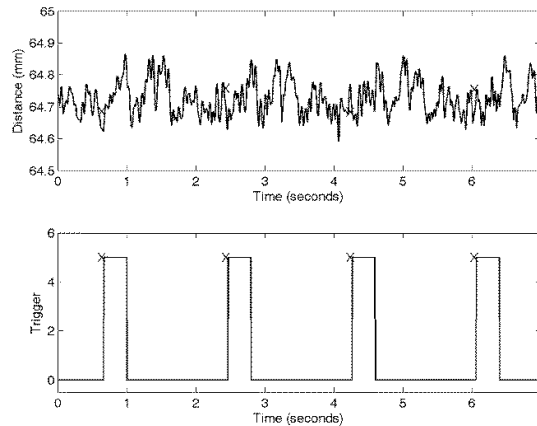


**Figure 7 Trigger signals**

The triggering is based on an optoelectric sensor measuring the change from a dark area to a light area on the shaft as it rotates. In this case, each shaft rotation takes 1.6 seconds

(37.5rpm). The data for each of the shaft revolutions acquired over the period can be separated as shown in Figure 8.

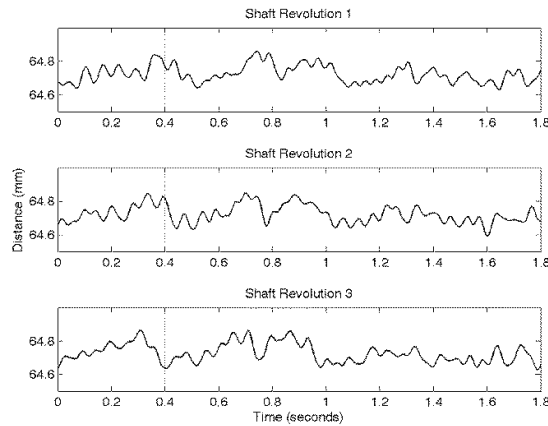


**Figure 8 Shaft revolution measurements**

Finally, the ensemble average is performed to calculate the average measurement per shaft revolution, for example the average value of the three points on each revolution at time 0.4 seconds on Figure 8, would give the ensemble average value at 0.4 seconds (denoted by “X” on Figure 9), reducing the multiple periods of data for each shaft revolution to a single period.

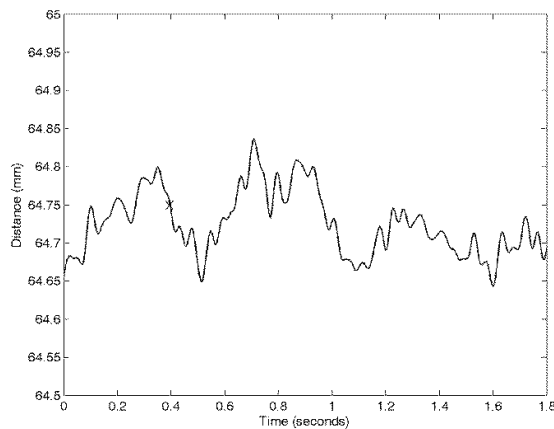


**Figure 9 Shaft revolution ensemble average**

The mean of the ensemble-averaged data, the measurement over a single revolution, is then used to calculate the distance from the laser to the shaft, 64.72mm in Figure 9. The difference in the mean value from a baseline (shaft aligned) value will then be used to estimate the amount of shaft misalignment as shown in Figure 10.

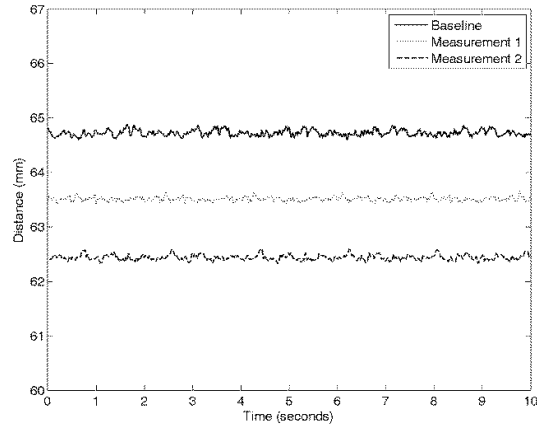


**Figure 10 Measurement change from baseline value**

The measurement can be converted to cylindrical coordinates and displayed as the distance to the surface of the 6mm diameter shaft as shown in Figure 11.

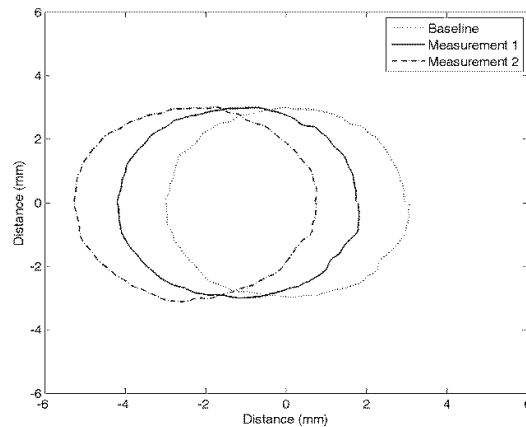


**Figure 11 Shaft change from baseline value**

The difference in shaft centers show the amount of shaft misalignment and fluctuations in shaft circumference are variations in the rotation. The negative values indicate that the misalignment is towards the position of the measurement laser (the distance is decreasing).

### 3.4 Results

After a baseline measurement was performed (on the aligned shaft), the level of shaft misalignment was increased by adjusting the lead screws on the test rig and the distance to the shaft was measured using the distance measurement lasers.

The results for the shaft misalignment tests will now be given. The results for misalignment test 1 and misalignment test 2 (measured at position *P3* on Figure 3) are shown in Figure 12 and the results for misalignment test 3 and misalignment test 4 (measured at position *P5* on Figure 3) are shown in Figure 13.

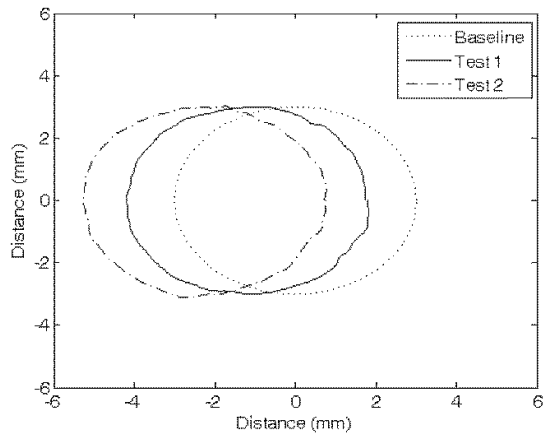


**Figure 12 Shaft position change for misalignment test 1 and misalignment test 2**

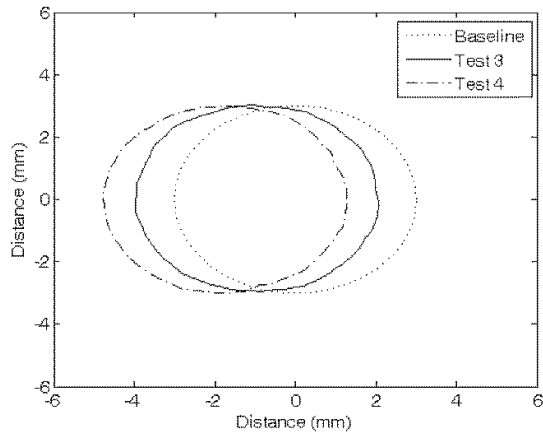


**Figure 13 Shaft position change for misalignment test 3 and misalignment test 4**

The results from these tests show that the increasing amounts of shaft misalignment can be identified, as the circles are shifted from the baseline value. As well as measuring the position at a single point on the shaft, by measuring the amount of misalignment at various positions on the shaft (moving a single distance measurement laser or using multiple distance measurement lasers), the type of shaft misalignment as shown in Figure 1 can be identified. The results for misalignment test 1 and misalignment test 2 (offset misalignment) are shown in Figure 14 and the results for misalignment test 3 and misalignment test 4 (angular misalignment) are shown in Figure 15.

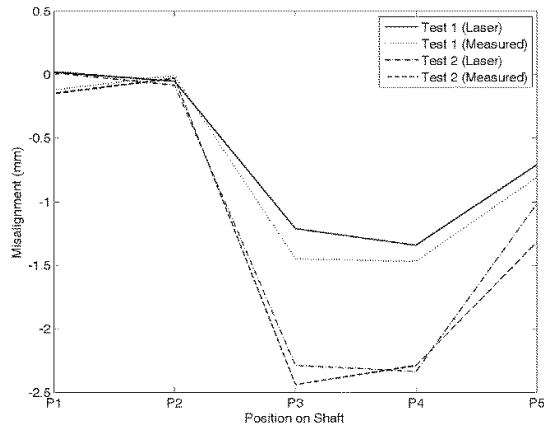


**Figure 14 Shaft misalignment results for misalignment test 1 and misalignment test 2 (offset misalignment)**

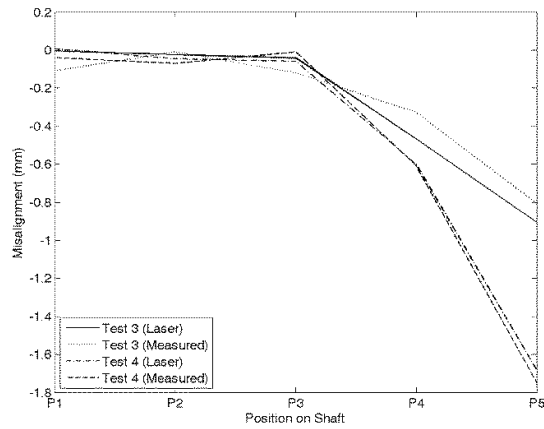


**Figure 15 Shaft misalignment results for misalignment test 3 and misalignment test 4 (angular misalignment)**

Figure 14 shows that the area of the shaft between positions  $P3$  and  $P4$ , attached to the first leadscrew, has been offset from the rest of the shaft as the amount of misalignment has been increased. Figure 15 shows that the angle of position  $P5$  has been increased as the second leadscrew is adjusted.

The distance measurements from the laser are also compared against manual distance measurements made using an electronic vernier caliper, as shown in Table 1, where both the measurement error and percentage error (in brackets) are given.

**Table 1 Error between laser measurement and manual measurement of shaft misalignment**

Test	P1	P2	P3	P4	P5
Misalignment test 1	-0.14mm (116%)	0.04mm (419%)	-0.24mm (16%)	-0.13mm (9%)	-0.10mm (12%)
Misalignment test 2	-0.16mm (108%)	0.05mm (177%)	-0.15mm (6%)	0.05mm (2%)	-0.30mm (23%)
Misalignment test 3	-0.11mm (96%)	0.01mm (135%)	-0.08mm (66%)	0.14mm (42%)	0.10mm (12%)
Misalignment test 4	-0.05mm (117%)	-0.02mm (34%)	0.05mm (500%)	-0.01mm (1%)	-0.06mm (4%)

As well as studying offset and angular types of shaft misalignment individually, the more realistic shaft misalignment can be studied by adjusting both leadscrews simultaneously, in misalignment test 5 and misalignment test 6, to add both types of shaft misalignment as shown in Figure 16. For comparison, the results of adding the individual amounts of offset and angular shaft misalignments are shown, indicating good agreement with this test result.

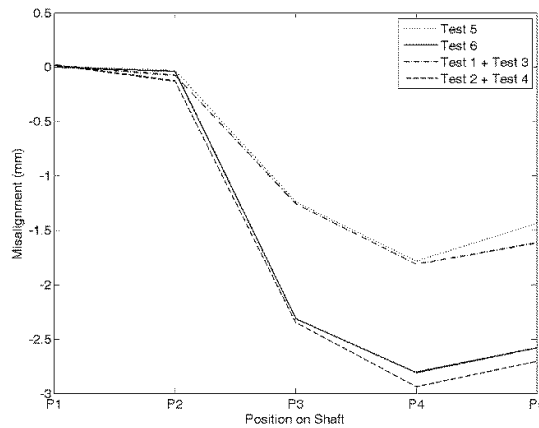


**Figure 16 Shaft misalignment results for misalignment test 5 and misalignment test 6 (offset and angular misalignment combined)**

These measurements give a visual representation of both the type and amount of shaft misalignment. The distance measurements can be used to perform the required machine movements to return the systems to the baseline aligned condition. In addition, in condition monitoring applications, the measurements can be used to trigger an alarm if they exceed a threshold value.

As well as measuring static values of shaft misalignment, the level of shaft misalignment was recorded as it was being adjusted over time (misalignment test 7). The result for the measured shaft misalignment (measured at position *P3* on Figure 3) is shown in Figure 17 and the corresponding shaft position changes over time (at one, two and three seconds) is shown in Figure 18.

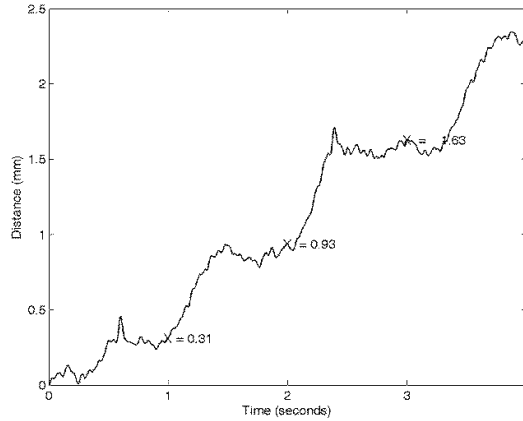


Figure 17 Shaft misalignment change over time for misalignment test 7

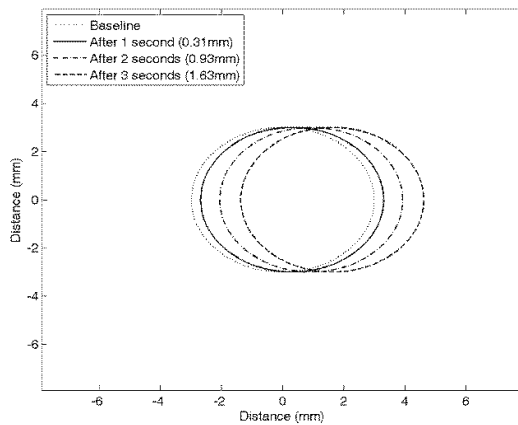


Figure 18 Shaft position change over time for misalignment test 7

This shows the main advantage over existing laser based shaft misalignment measurement methods, this is a non-contact method and it can be used while the rotating machine is in operation (unlike existing shaft misalignment measuring tools, which are attached to the shaft so the machine should be stopped). This on-line measurement procedure is a requirement for condition monitoring, as it can detect changes in shaft misalignment over time.

#### 4 Conclusions and future work

A requirement exists in industry for rapid and reliable techniques to measure shaft misalignment, so that the condition of the rotating machines can be monitored and the shafts can be adjusted to achieve proper alignment. To achieve this, this work has presented a novel laser based measurement method for shaft misalignment monitoring. This uses a commercially available laser distance measuring device to measure the change in distance to a rotating shaft caused by the presence of shaft misalignment. This has advantages over existing misalignment measurement methods of being non-contact and suitable for on-line operation. Several misalignment tests have been performed to demonstrate the feasibility of

the technique. Variations in misalignment have been identified as well as identification of the two common types of misalignment (offset and angular) and the measurement of changes in shaft misalignment over time.

This technique has been used to measure shaft misalignment distances of between 0.5mm and 2.5mm on an experimental test rig. These are larger than practical shaft misalignment tolerances, which are usually based on the rotational speed of the machine, varying between 0.02mm and 0.3mm [45], future work could be performed to measure alignment at this greater precision with higher specification laser measurement equipment (the resolution of the current laser measurement system is 0.06mm) as the feasibility of the technique has been demonstrated. It would also be useful to extend this work to data acquisition over long periods and machine diagnostics based on the acquired shaft misalignment measurements, plus investigation of the system performance in harsh environments.

### **Acknowledgements**

This work was supported by UK Engineering and Physical Sciences Research Council (EPSRC) Centre for Through-life Engineering Services (EP/1033246/1, Project SC006) and EPSRC Impact Acceleration Award (EP/K50336811), Royal Academy of Engineering Newton Collaborative Research Programme (NRCP 1415 91) and Royal Academy of Engineering Distinguished Visiting Fellowship (DVF 1415 2 17).

### **References**

- [1] R.K. Mobley, Maintenance Fundamentals, Elsevier Inc., 2004.
- [2] S. Ebersbach, Artificial intelligence system for integrated wear debris and vibration analysis in machine condition monitoring, School of Engineering, James Cook University, 2007.
- [3] J.K. Sinha, K. Elbhah, A future possibility of vibration based condition monitoring, Mechanical Systems and Signal Processing, 34 (2013) 231-240.
- [4] Y. Lei, J. Lin, Z. He, M.J. Zuo, A review on empirical mode decomposition in fault diagnosis of rotating machinery, Mechanical Systems and Signal Processing, 35 (2013) 108-126.
- [5] P. Scanlon, D.F. Kavanagh, F.M. Boland, Residual Life Prediction of Rotating Machines Using Acoustic Noise Signals, IEEE Transactions on Instrumentation and Measurement, 62 (2013) 95-108.
- [6] P. Tavner, L. Ran, J. Penman, H. Sedding, Condition Monitoring of Rotating Electrical Machines, The Institution of Engineering and Technology, London, 2008.
- [7] Y. Amirat, M.E.H. Benbouzid, E. Al-Ahmar, B. Bensaker, S. Turri, A brief status on condition monitoring and fault diagnosis in wind energy, Renewable and Sustainable Energy Reviews, 13 (2009) 2629-2636.
- [8] J.F. Manwell, J.G. McGowan, A.L. Rogers, Wind Energy Explained Theory, Design and Application, John Wiley & Sons Ltd, Chichester, 2009.
- [9] GL Garrad Hassan, Offshore Wind - Operations & Maintenance opportunities in Scotland - An insight into opportunities, Scottish Enterprise and GL Garrad Hassan.
- [10] T.H. Patel, A.K. Darpe, Experimental investigations on vibration response of misaligned rotors, Mechanical Systems and Signal Processing, 23 (2009) 2236-2252.

- [11] J. Piotrowski, Shaft Alignment Handbook, CRC Press, 2007.
- [12] Y. Fang, H. Cho, M. Jeong, Health monitoring of a shaft transmission system via hybrid models of PCR and PLS, in: J. Ghosh, D. Lambert, D. Skillicorn, J. Srivastava (Eds.) Sixth SIAM International Conference on Data Mining, Bethesda, Maryland, 2006.
- [13] A. Kr Jalan, A.R. Mohanty, Model based fault diagnosis of a rotor-bearing system for misalignment and unbalance under steady-state condition, Journal of Sound and Vibration, 327 (2009) 604-622.
- [14] L. Arebi, F. Gu, A. Ball, A comparative study of misalignment detection using a novel Wireless Sensor with conventional Wired Sensors, 25th International Congress on Condition Monitoring and Diagnostic Engineering, IOP Publishing, Huddersfield, UK, 2012.
- [15] J.M. Vance, Rotordynamics of Turbomachinery, John Wiley & Sons, Inc., 1988.
- [16] D.L. Dewell, L.D. Mitchell, Detection of a Misaligned Disk Coupling Using Spectrum Analysis, Journal of Vibration, Acoustics Stress and Reliability in Design 106 (1984) 9-16.
- [17] M. Xu, R.D. Marangoni, Vibration Analysis Of A Motor-Flexible Coupling-Rotor System Subject To Misalignment And Unbalance, Part I: Theoretical Model And Analysis, Journal of Sound and Vibration, 176 (1994) 663-679.
- [18] M. Xu, R.D. Marangoni, Vibration Analysis Of A Motor-Flexible Coupling-Rotor System Subject To Misalignment And Unbalance, Part II: Experimental Validation, Journal of Sound and Vibration, 176 (1994) 681-691.
- [19] P.N. Saavedra, D.E. Ramírez, Vibration analysis of rotors for the identification of shaft misalignment Part 2: Experimental validation, Proceedings of the Institution of Mechanical Engineers, Part C: Journal of Mechanical Engineering Science, 218 (2004) 987-999.
- [20] S.B. Chaudhury, S. Gupta, Online Identification of AC Motor Misalignment Using Current Signature Analysis and Modified K-Mean Clustering Technique, IEEE International Conference on Industrial Technology, 2006., Mumbai, 2006, pp. 2331-2336.
- [21] A.K. Verma, S. Sarangi, M.H. Kolekar, Shaft Misalignment Detection using Stator Current Monitoring, International Journal of Advanced Computer Research, 3 (2013) 305-309.
- [22] W.T. Thomson, M. Fenger, Current signature analysis to detect induction motor faults, IEEE Industry Applications Magazine, 7 (2001) 26-34.
- [23] J.M. Bossio, G.R. Bossio, C.H. De Angelo, Angular Misalignment in Induction Motors with Flexible Coupling, 35th Annual Conference of IEEE Industrial Electronics, 2009, Porto, 2009, pp. 1033-1038.
- [24] G.R. Rameshkumar, B.V.A. Rao, K.P. Ramachandran, Coast Down Time Analysis to Analyze the Effect of Misalignment in Rotating Machinery, International Journal of Engineering and Advanced Technology, 1 (2012) 149-156.
- [25] S.M. Kim, J.H. Suh, J.S. Im, S.B. Kim, S.B. Kim, A Smart Memory Type of Data Acquisition System for Shaft Misalignment Maintenance, Journal of Mechanical Science and Technology, 19 (2005) 15-27.
- [26] M.A. Hotait, D. Talbot, A. Kahraman, An Investigation of the Influence of Shaft Misalignment on Bending Stresses of Helical Gears with Lead Crown, Gear Technology, 2008, pp. 54-62.
- [27] A.G. Fulzele, V.G. Arajpure, P.P. Holay, N.M. Patil, Condition monitoring of shaft of single-phase induction motor using optical sensor, Mechanical Systems and Signal Processing, 29 (2012) 428-435.

- [28] A.S. Sekhar, B.S. Prabhu, Effects of coupling misalignment on vibrations of rotating machinery, *Journal of Sound and Vibration*, 185 (1995) 655-671.
- [29] H.-W. Cho, M.K. Jeong, Enhanced prediction of misalignment conditions from spectral data using feature selection and filtering, *Expert Systems with Applications*, 35 (2008) 451-458.
- [30] W. Yang, P.J. Tavner, Empirical mode decomposition, an adaptive approach for interpreting shaft vibratory signals of large rotating machinery, *Journal of Sound and Vibration*, 321 (2009) 1144-1170.
- [31] J. Giannone, Laser-optical shaft alignment cuts energy costs, *World Pumps*, 1995 (1995) 22-24.
- [32] V. Hariharan, P.S.S. Srinivasan, Vibration analysis of misaligned shaft-ball bearing system, *Indian Journal of Science and Technology*, 2 (2009) 45-50.
- [33] R.B. McMillan, *Rotating machinery: practical solutions to unbalance and misalignment*, The Fairmont Press, Inc., 2004.
- [34] M.M. Hodowanec, Effects of Coupling Installation on Motor Performance, *IEEE Industry Applications Magazine*, (1997) 70-77.
- [35] Huco Engineering Industries Ltd, *Flex-P Double Loop Couplings with Stainless Steel Hubs*.
- [36] M.-A. Beeck, W. Hentschel, Laser metrology - a diagnostic tool in automotive development processes, *Optics and Lasers in Engineering*, 34 (2000) 101-120.
- [37] I. Besic, N. van Gestel, J.-P. Kruth, P. Bleys, J. Hodolic, Accuracy improvement of laser line scanning for feature measurements on CMM, *Optics and Lasers in Engineering*, 49 (2011) 1274-1280.
- [38] S.H. Wang, C.J. Jin, C.J. Tay, C. Quan, H.M. Shang, Design of an optical probe for testing surface roughness and micro-displacement, *Precision Engineering*, 25 (2001) 258-265.
- [39] P. Cheng, M.S.M. Mustafa, B. Oelmann, Contactless Rotor RPM Measurement Using Laser Mouse Sensors, *IEEE Transactions on Instrumentation and Measurement*, 61 (2012) 740-748.
- [40] A.K.S. Jardine, D. Lin, D. Banjevic, A review on machinery diagnostics and prognostics implementing condition-based maintenance, *Mechanical Systems and Signal Processing*, 20 (2006) 1483-1510.
- [41] National Instruments Corporation, *TSA Moving Average VI*.
- [42] R. Henderson, Note on Graduation by Adjusted Average, *Transaction of the Actuarial Society of America*, 17 (1916) 43-48.
- [43] S. Boslaugh, P.A. Watters, *Statistics in a Nutshell*, O'Reilly Media, Inc., Sebastopol, CA, 2008.
- [44] R.M. Chervin, Estimates of First- and Second-Moment Climate Statistics in GCM Simulated Climate Ensembles, *Journal of the Atmospheric Sciences*, 37 (1980) 1889-1902.
- [45] Pruftechnik Ltd, *A Practical Guide to Shaft Misalignment*, Pruftechnik, 2002.